



CT texture analysis of pancreatic cancer

Kumar Sandrasegaran¹ · Yuning Lin^{1,2} · Michael Asare-Sawiri^{1,3} · Tai Taiyini¹ · Mark Tann¹

Received: 17 April 2018 / Revised: 15 June 2018 / Accepted: 13 July 2018 / Published online: 16 August 2018
© European Society of Radiology 2018

Abstract

Objectives We investigated the value of CT texture analysis (CTTA) in predicting prognosis of unresectable pancreatic cancer.

Methods Sixty patients with unresectable pancreatic cancers at presentation were enrolled for post-processing with CTTA using commercially available software (TexRAD Ltd, Cambridge, UK). The largest cross-section of the tumour on axial CT was chosen to draw a region-of-interest. CTTA parameters (mean value of positive pixels (MPP), kurtosis, entropy, skewness), arterial and venous invasion, metastatic disease and tumour size were correlated with overall and progression-free survivals.

Results The median overall and progression-free survivals of cohort were 13.3 and 7.8 months, respectively. On multivariate Cox proportional hazard regression analysis, presence of metastatic disease at presentation had the highest association with overall survival ($p = 0.003$ – 0.05) and progression-free survival ($p < 0.001$ to $p = 0.004$). MPP at medium spatial filter was significantly associated with poor overall survival ($p = 0.04$). On Kaplan–Meier survival analysis of CTTA parameters at medium spatial filter, MPP of more than 31.625 and kurtosis of more than 0.565 had significantly worse overall survival ($p = 0.036$ and 0.028 , respectively).

Conclusions CTTA features were significantly associated with overall survival in pancreas cancer, particularly in patients with non-metastatic, locally advanced disease.

Key Points

- CT texture analysis is easy to perform on contrast-enhanced CT.
- CT texture analysis can determine prognosis in patients with unresectable pancreas cancer.
- The best predictors of poor prognosis were high kurtosis and MPP.

Keywords Tomography, X-Ray Computed · Pancreas cancer · Survival analysis · Neoplasm invasion · Neoplasm metastases

Abbreviations

CTTA	CT texture analysis
MPP	Mean value of positive pixels
NCCN	National Comprehensive Cancer Network in USA
SSF	Spatial scaling factor

Introduction

Pancreatic cancer is the fourth leading cause of cancer-related deaths in men and women in the USA. Surgical resection with negative margins (R0 resection) is the only potentially curative therapy for pancreatic cancer. However, only 10–15% of patients will qualify for radical pancreatic resection. The rest of the patients have locally advanced (unresectable) disease (30–40%) or metastatic disease (50–60%) [1–3]. Survival in pancreatic cancer is generally dismal. Those who undergo curative resection and successful adjuvant chemotherapy have a median survival of 29 months [4, 5]. Locally advanced and metastatic disease at presentation correlate with median survivals of 11 and 6 months, respectively [5]. These two groups are considered distinct from resectable and borderline resectable cancers by the National Comprehensive Cancer Network (NCCN) [6]. These groups of patients are primarily treated with chemoradiotherapy.

✉ Kumar Sandrasegaran
ksandras@iupui.edu

¹ Department of Radiology, Indiana University School of Medicine, 550 N. University Blvd., UH 0279, Indianapolis, IN 46202, USA

² Department of Medical Imaging, Fuzhou General Hospital, Fuzhou, China

³ Hope Radiation Cancer, Panama City, FL, USA

As we move towards an era of customised cancer care, the more information we may obtain about a tumour, the better we can tailor the therapy for the patient. Heterogeneity within a tumour is one such piece of information. Tumour heterogeneity may be due to genomic variations and altered tumour microenvironment, resulting in regions of differential hypoxia, cellular density and angiogenesis [7, 8]. Such heterogeneity is associated with higher histological grades of malignancy, increased metastatic potential and resistance to chemotherapy or radiotherapy [9–15]. Filtration–histogram-based CT texture analyses (CTTA) use spatial filters that select for imaging features over larger scales (typically 1–6 mm) and histogram-based quantification reflects different components (object size, number, density) of tumour heterogeneity. This technique of CTTA reduces the effect of photon noise while enhancing biologic heterogeneity [16–18]. CTTA has been able to predict prognosis or treatment response in lung, oesophageal, colorectal and renal cancers as well as in sarcoma [18–25]. There have been no prior publications regarding the role of CTTA in predicting outcomes of unresectable pancreatic cancer. The aim of this study was to determine its value in predicting the survival in patients with unresectable pancreatic cancer.

Methods

Patients

This retrospective study was approved by the institutional review board (IRB) with waiver of informed patient consent. The study was Health and Insurance Portability Accountability Act (HIPAA)-compliant. Review of the institutional radiology databases for the period January 2007 to December 2014 revealed 126 patients with pancreatic cancer. Patients with unresectable pancreatic cancer (cohort $n = 60$) were selected. The exclusion criteria and derivation of the study cohort are shown in Fig. 1. The patients' therapy followed established NCCN protocols [6], with locally advanced cancers being treated with gemcitabine-based chemotherapy and stereotactic body radiation therapy. Patients with metastatic disease were primarily treated with FOLFIRINOX-based chemotherapy. Additional chemotherapy agents were used in patients with good ECOG (Eastern Cooperative Oncology Group) status.

CT examination

All patients underwent standard diagnostic contrast-enhanced CT examinations of the abdomen in venous phase only ($n = 34$) or late arterial (parenchymal) and venous phases ($n = 26$). CT studies were performed with multislice CT scanner (Phillips Healthcare, Best, Netherlands) using similar

protocols: 120 kVp, 180–450 mA with tube current modulation, matrix of 512, field of view of 380–500 mm, and 4- or 5-mm reconstructed section thickness after intravenous injection of 120 mL of 370 mg of iodine/mL of iopamidol (Isovue 370, Bracco Healthcare, Princeton, NJ) at 3 mL/s. The late arterial and portal venous phases were obtained 35 and 75 s after commencement of contrast agent administration.

Image analysis

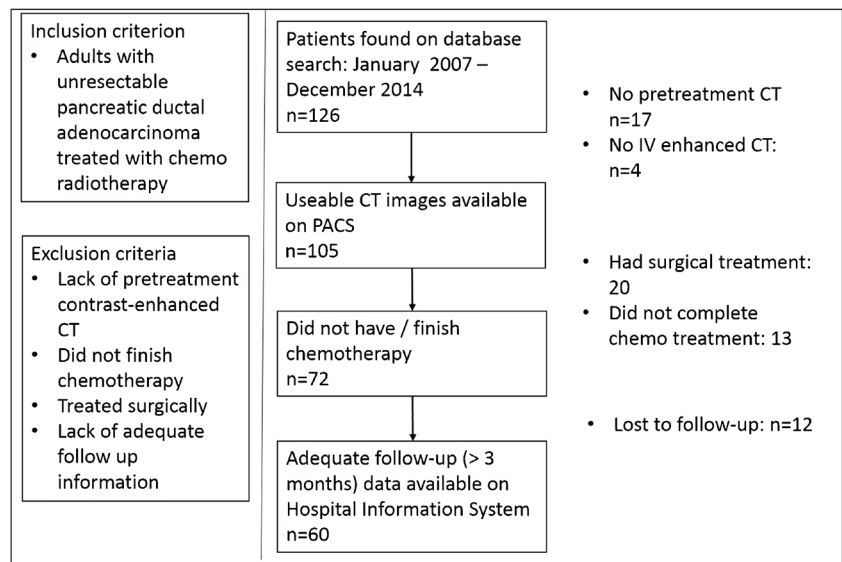
Analysis was performed using a commercially available CTTA research software (TexRAD Ltd, Cambridge, UK), for which dedicated training was provided to the study members by the vendor. All data was controlled by the authors. An abdominal radiologist with 5 years' training (LY) selected the axial image in the pretreatment venous phase that showed the largest cross-section of the primary tumour. This radiologist had used CTTA software for a prior study of 130 patients [26]. This image was anonymised for all patient data and labelled with a random number. The single image for each patient was uploaded to the server housing the software. The software package was used to manually draw a polygon region of interest (ROI) within the tumour (close to the tumour margin). The software automatically applied a threshold to exclude pixels with Hounsfield attenuation values less than -50, thereby excluding gas or fat at the margins of the mass.

CTTA methodology using the filtration–histogram technique has been described elsewhere [18, 27–29]. Once ROIs are obtained, the CTTA software modifies the pixel data using several Laplacian spatial scaling factors (SSF), which extracts and enhances features of different sizes (mm) ranging from no filter (labelled SSF 0 which is nothing but the conventional image), fine (SSF = 2 mm), medium (SSF = 4 mm) and coarse (SSF = 6 mm) texture scales. The fine filter tends to enhance tissue parenchymal features, while medium to coarse filters enhanced vascular features [12]. The filtration step creates derived filtered maps, which are quantified to yield four parameters from histogram and statistical analysis: mean value of positive pixels (average brightness considering only the positive pixel values), entropy (irregularity of pixel intensities), kurtosis (peakedness or sharpness of the pixel distribution) and skewness (asymmetry of pixel distribution). The mathematical process of calculating these parameters has been previously described [21, 24, 30].

Statistical analysis

Overall survival (time from diagnosis to death from any cause) and progression-free survival were calculated. Two-step multivariate Cox proportional hazards regression models were fitted to examine the associations of the CTTA parameters and survival. First, multivariate Cox proportional hazards models were fitted in which the survival time was regressed

Fig. 1 Flowchart of study population. *IV* intravenous, *PACS* picture archiving and communication system



on the four texture parameters (entropy, kurtosis, MPP and skewness). Next, the conventional imaging variables of arterial invasion, venous invasion, metastases at presentation and tumour size were included into the Cox models as covariates. Texture parameters that were found to be significant ($p < 0.05$) or trending to significance ($0.05 < p < 0.10$) in the Cox models were dichotomised on the basis of median values. Although $p < 0.05$ was considered to indicate a significant difference, a stepwise Holm–Bonferroni procedure was used to reduce the potential for type I errors arising from multiple comparisons [31]. Log-rank tests were performed to compare the survival times between the groups with above-median and below-median values for the CTTA parameters. Kaplan–Meier graphs of the survival times were plotted. All analyses were performed using SAS v9.4 (SAS Institute Inc., Cary, NC).

Results

Patients and tumours

The patients’ epidemiology and tumour characteristics are shown in Table 1. Most patients (88%) had cancer in the head of pancreas. Twenty-five patients had metastatic disease at presentation, the clear majority of which were in the liver (92%). Thirty-five patients had advanced vascular invasion. Since the database search was for CT studies in which pancreatic cancer was reported, isodense tumours were excluded from the cohort.

Survival data

The median overall survival and progression-free survival in the cohort ($n = 60$) were 13.3 and 7.8 months, respectively.

Table 2 gives the mean and standard deviation of CTTA parameters at different spatial filters for patients with higher and lower than median overall survival. Patients with worse prognosis had lower entropy, higher mean positive pixel value (MPP) and higher kurtosis.

Table 1 Patient and tumour characteristics

Characteristic	Number of patients ($n = 60$)
Age (mean, range in years)	61.3 (40–81)
Gender	
Male	37
Female	23
Tumour Location	
Head	53
Body	4
Tail	3
Metastases at presentation	
None	35
Liver	23
Lung	3
Adrenal	4
Others (kidney, omentum)	2
Veins involved	
None	37
Portal vein	16
Superior mesenteric vein	16
Arteries invaded	
None	38
Celiac artery	9
Superior mesenteric artery	17
Hepatic artery	8

Table 2 CTTA parameters and overall survival

		< Median OS	> Median OS	<i>p</i>
SSF 0	Entropy	4.38 (0.21)	4.46 (0.17)	0.119
	MPP	58.07 (14.83)	56.72 (9.91)	0.266
	Skewness	0.126 (0.323)	0.063 (0.248)	0.403
	Kurtosis	0.221 (0.426)	0.178 (0.445)	0.706
SSF 2	Entropy	4.69 (0.33)	4.88 (0.33)	0.084
	MPP	38.15 (12.58)	37.69 (10.99)	0.616
	Skewness	−0.049 (0.388)	−0.050 (0.355)	0.986
	Kurtosis	0.086 (0.648)	−0.050 (0.605)	0.407
SSF 4	Entropy	4.91 (0.43)	4.97 (0.31)	0.610
	MPP	34.83 (14.38)	28.77 (10.46)	0.051
	Skewness	−0.620 (1.018)	−0.314 (0.665)	0.174
	Kurtosis	2.47 (4.43)	0.83 (1.53)	0.053
SSF 6	Entropy	4.81 (0.73)	4.88 (0.45)	0.656
	MPP	28.26 (17.90)	27.98 (10.69)	0.943
	Skewness	−0.397 (0.812)	−0.2217 (0.598)	0.345
	Kurtosis	0.820 (2.031)	0.172 (0.983)	0.121

Table shows mean (standard deviation) of CTTA parameters for patients with less than (<) and higher than (>) median overall survival (OS)

SSF spatial scaling factors, SSF 0 no filtration, SSF 2 fine filtration, SSF 4 medium filtration, SSF 6 coarse filtration

MPP and Kurtosis at SS4 show significant differences in Overall Survival (OS)

Table 3 gives the result of univariate Cox proportional hazard regression analysis for overall and progression-free survivals. In this analysis, the presence of metastases had the greatest association with both overall and progression-free survivals ($p = 0.017$ and 0.002 , respectively). Venous invasion had a significant association with overall survival ($p = 0.048$). The only CTTA parameter to have a substantial, but not significant, association with overall survival was kurtosis at SSF 4 ($p = 0.052$).

Tables 4 and 5 give the results of multivariate Cox proportional hazard regression analysis for overall and progression-free survivals, respectively. The best associations with overall survival were found with metastatic disease, venous invasion and arterial invasion, in that order. Mean positive pixel value (MPP) at SSF4 (medium texture) was also significantly associated with overall survival ($p = 0.042$). The other CTTA parameters and tumour size were not associated with overall survival. Progression-free survival was only significantly associated with the presence of metastases. Vascular invasion, tumour size and CTTA parameters were not significant indicators of progression-free survival.

Figure 2a gives the Kaplan–Meier survival curves for overall survival in patients with high and low MPP at medium spatial filter. Those with MPP more than 31.625 had overall survival below the median for the cohort. Similarly, patients with high kurtosis at medium spatial filter also had poor overall survival (Fig. 2b). There was no significant difference

Table 3 Univariate Cox proportional hazard regression for survival

Variables	OS			PFS		
	SSF	HR (95% CI)	<i>p</i>	HR (95% CI)	<i>p</i>	
Entropy	0	0.76 (0.20–2.96)	0.692	0.53 (0.15–1.92)	0.336	
	2	0.54 (0.25–1.17)	0.119	0.65 (0.31–1.38)	0.263	
	4	1.55 (0.71–3.38)	0.273	1.05 (0.50–2.20)	0.900	
	6	1.24 (0.72–2.13)	0.431	1.06 (0.63–1.79)	0.814	
	Kurtosis	0	1.24 (0.67–2.27)	0.496	1.69 (0.94–3.04)	0.082
		2	1.08 (0.72–1.63)	0.706	1.25 (0.86–1.82)	0.251
4		1.08 (1.00–1.16)	0.052	1.03 (0.96–1.11)	0.420	
6		1.17 (0.98–1.40)	0.081	1.06 (0.90–1.25)	0.483	
MPP	0	1.00 (0.97–1.02)	0.836	1.00 (0.97–1.02)	0.711	
	2	1.00 (0.98–1.02)	0.922	1.00 (0.98–1.02)	0.985	
	4	1.02 (1.00–1.04)	0.108	1.00 (0.98–1.03)	0.762	
	6	1.01 (0.99–1.03)	0.305	1.00 (0.98–1.03)	0.648	
	Skewness	0	1.45 (0.53–3.92)	0.468	1.35 (0.47–3.88)	0.574
		2	0.87 (0.43–1.74)	0.688	1.39 (0.68–2.86)	0.370
4		0.86 (0.63–1.17)	0.331	0.97 (0.70–1.33)	0.836	
6		0.91 (0.61–1.35)	0.646	1.06 (0.72–1.56)	0.766	
Vein invasion		1.77 (1.00–3.10)	0.048	1.14 (0.66–1.98)	0.627	
Arterial invasion		0.85 (0.50–1.45)	0.549	0.73 (0.43–1.24)	0.248	
Size of tumour		1.1 (0.94–1.29)	0.235	1.02 (0.88–1.18)	0.814	
Metastases		1.93 (1.12–3.30)	0.017	2.32 (1.36–3.96)	0.002	

OS overall survival, PFS progression-free survival, HR (95% CI) hazard ratio (95% confidence interval), SSF spatial scaling factor (see text), MPP mean positive pixel value

between MPP ($p = 0.390$) or kurtosis ($p = 0.712$) for patients with and without metastatic disease.

Discussion

Heterogeneity within a tumour may be due to multiple factors, including variable genomic expression and angiogenesis. Heterogeneity in blood flow may result in foci of hypoxia and micronecrosis, which have been shown to result in impaired response to chemotherapy and radiotherapy [7, 13]. Until recently imaging assessment of tumour texture has been primarily qualitative and compounded by variation in photon noise. CTTA was developed as a technique to give quantitative parameters of tumour heterogeneity, without being affected by photon noise [16–18]. Several articles have previously discussed the CTTA parameters [27, 28, 32]. Briefly, kurtosis is related to the peakedness of the pixel distribution curve in the region-of-interest. A positive or negative kurtosis indicates a histogram that is either more or less peaked, respectively, than a Gaussian distribution. Entropy is a measure of random irregularity in the distribution of pixel densities. In general, tumours with increased histological heterogeneity have CTTA parameters of higher entropy, higher kurtosis and positive

Table 4 Multivariate Cox proportional hazard regression for overall survival

Variables	SSF 0		SSF 2		SSF 4		SSF 6	
	HR (95% CI)	<i>p</i>	HR (95% CI)	<i>p</i>	HR (95% CI)	<i>p</i>	HR (95% CI)	<i>p</i>
Entropy	0.82 (0.19–3.55)	0.795	0.63 (0.26–1.49)	0.291	0.57 (0.16–2.02)	0.382	0.88 (0.41–1.86)	0.730
Kurtosis	1.05 (0.53–2.09)	0.886	0.93 (0.58–1.50)	0.759	1.13 (0.96–1.33)	0.134	1.17 (0.88–1.55)	0.282
MPP	1.00 (0.97–1.02)	0.831	1.00 (0.97–1.03)	0.845	1.04 (1.00–1.08)	0.042	1.02 (0.99–1.06)	0.143
Skewness	1.52 (0.49–4.73)	0.471	1.18 (0.50–2.77)	0.708	1.22 (0.68–2.19)	0.504	1.21 (0.71–2.03)	0.483
Vein invasion	3.22 (1.45–7.14)	0.004	2.91 (1.33–6.39)	0.008	2.53 (1.14–5.59)	0.022	2.6 (1.16–5.82)	0.020
Arterial invasion	1.40 (1.18–1.89)	0.025	1.44 (1.20–1.97)	0.041	1.58 (0.26–2.28)	0.177	1.50 (0.23–2.11)	0.088
Size of tumour	1.13 (0.95–1.35)	0.172	1.13 (0.95–1.34)	0.154	1.07 (0.88–1.29)	0.497	1.09 (0.89–1.33)	0.418
Metastases	1.77 (1.00–3.13)	0.050	1.83 (1.00–3.34)	0.051	2.5 (1.37–4.56)	0.003	2.35 (1.28–4.31)	0.006

HR (95% CI) hazard ratio (95% confidence interval), SSF spatial scaling factor (see text), MPP mean positive pixel value

skewness. The spatial scaling factor (SSF) values used in this study were 2 mm, 4 mm and 6 mm, highlighting fine, medium and coarse filtrations, respectively. Unfiltered images (SSF 0) corresponded to conventional CT images.

Prior studies have assessed the prediction of prognosis using CTTA parameters in head and neck squamous [22], lung [20, 23], oesophageal [12, 21], colorectal [18, 33] cancers, sarcoma [34] and melanoma [35]. Studies have found that high entropy, suggesting increased tumour heterogeneity, is associated with worse outcomes in oesophageal cancer [12, 21], metastatic colorectal cancer [18, 33] and non-small cell lung cancer [23]. High mean value of positive pixels was found to be associated with high tumour grade in colorectal cancer [33]. Positive skewness was associated with adverse outcome in metastatic colorectal cancer [18], head and neck cancer [22] and non-small cell lung cancer [23]. High kurtosis was associated with worse outcomes in soft tissue sarcoma [34]. In concordance with prior studies, we found that higher mean positive pixel values and kurtosis were seen in patients with poor overall survival.

Pancreatic cancer has a substantially worse prognosis than the other cancers investigated with CTTA. We chose a relatively homogenous group of inoperable pancreatic cancer patients for

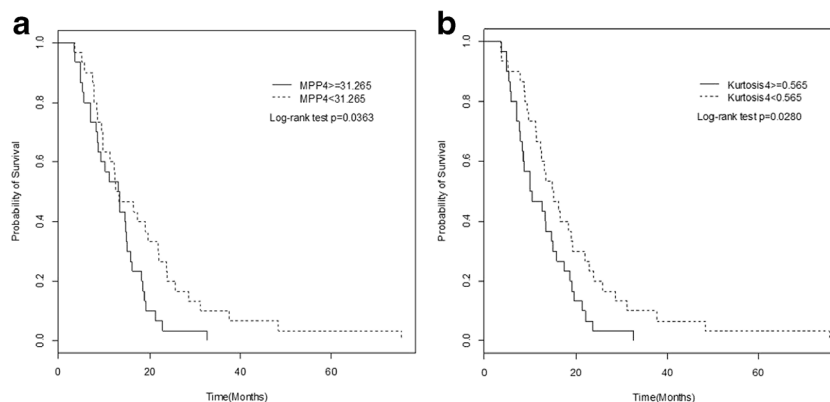
investigation. We found that metastatic disease at presentation had the most significant association with overall survival and progression-free survival, on multivariate Cox proportional hazard regression analysis. The next highest associations with survival were venous invasion and arterial invasion. This is in keeping with mean survival of 6 and 11 months for pancreatic cancer patients with metastatic disease and local vascular invasion, respectively [4, 5]. Tumour size was not significantly correlated with poor outcomes. The only CTTA parameter to show significance on multivariate Cox proportional hazard analysis was MPP (*p* = 0.042). High MPP was associated with worse survival. To our knowledge only one other paper has addressed the role of CTTA in determining prognosis in pancreatic cancer [36]. That paper reported that, in 30 patients with resectable pancreatic cancer, CTTA features of entropy, uniformity and mean intensity were significantly different between the cancer and surrounding normal parenchyma. However, the paper reported that CTTA features, such as mean intensity and entropy, as well as tumour size, did not predict overall survival. The discrepancy in results between that paper and ours may be due to different patient populations that were studied (resectable pancreatic cancer versus

Table 5 Multivariate Cox proportional hazard regression for progression-free survival

Variables	SSF 0		SSF 2		SSF 4		SSF 6	
	HR (95% CI)	<i>p</i>	HR (95% CI)	<i>p</i>	HR (95% CI)	<i>p</i>	HR (95% CI)	<i>p</i>
Entropy	0.58 (0.14–2.37)	0.447	0.51 (0.23–1.10)	0.086	0.97 (0.21–4.56)	0.973	0.9 (0.40–2.03)	0.801
Kurtosis	1.69 (0.87–3.28)	0.123	1.53 (0.97–2.41)	0.066	1.12 (0.95–1.32)	0.174	1.21 (0.90–1.63)	0.205
MPP	0.99 (0.96–1.01)	0.355	1.01 (0.98–1.04)	0.566	1.01 (0.96–1.05)	0.755	1.02 (0.99–1.06)	0.215
Skewness	1.29 (0.42–4.01)	0.655	1.57 (0.71–3.49)	0.267	1.55 (0.81–2.96)	0.185	1.74 (0.94–3.22)	0.077
Vein invasion	2.03 (0.93–4.40)	0.074	1.88 (0.88–4.02)	0.105	1.54 (0.70–3.41)	0.282	1.49 (0.67–3.33)	0.333
Arterial invasion	0.47 (0.22–1.03)	0.061	0.5 (0.22–1.10)	0.084	0.61 (0.27–1.37)	0.228	0.56 (0.25–1.29)	0.174
Size of tumour	1.01 (0.85–1.19)	0.941	1.06 (0.91–1.23)	0.437	1.03 (0.86–1.23)	0.766	1.07 (0.89–1.29)	0.455
Metastases	2.45 (1.39–4.31)	0.002	2.42 (1.32–4.43)	0.004	2.6 (1.45–4.66)	0.001	3.1 (1.66–5.79)	< 0.001

HR (95% CI) hazard ratio (95% confidence interval), SSF spatial scaling factor (see text), MPP mean positive pixel value

Fig. 2 Kaplan–Meier survival curves show a significant difference in overall survival for **a** mean value of positive pixels (MPP), **b** kurtosis of the pixel distribution histogram with medium spatial filter (SSF 4)



unresectable disease). There were also methodological differences in texture analysis of the two papers.

Kaplan–Meier statistics showed that texture parameters may be helpful in predicting prognosis in patients with pancreatic cancer. Patients with high MPP (of more than 31.6) and high kurtosis (of more than 0.565) at medium spatial filter had worse prognosis. Unlike prior studies, we did not find the other CTTA parameters, particularly entropy, to be associated with survival. These results may be explained by methodological differences between our study and some of the previously published studies. The prognosis of pancreatic cancer is abysmal, and instead of evaluating 3-year or 5-year survival, we investigated overall survival. Treatment regimens in prior papers varied including surgery [34] or chemotherapy [18, 22, 23]. Our patients only had chemotherapy and radiotherapy. We not only assessed texture parameters, but also conventional CT findings, such as tumour size, presence of metastatic disease and local vascular invasion, which are known to affect prognosis. Finally, it is possible that CTTA parameters of squamous cancers in the head and neck and oesophagus may be different from those of adenocarcinoma.

We are aware of some limitations to our study. The study is retrospective, and the number of patients is small. Another limitation is that we used the axial slice with maximum tumour dimensions to perform analysis rather than analysing multiple sections through the whole tumour. One study showed that two-dimensional texture analysis gives adequate results, though multislice volume analysis may be more representative of tumour [14]. We believe that more standardised methods of CT scanning and rigorous statistical analysis may be required in the future if CT texture analysis is to find widespread clinical use. It may be particularly useful to determine which texture parameters and at which spatial filters should be analysed for a particular tumour. We did not use MRI for determination of liver metastases since this is not the standard-of-care in the USA, and the NCCN considers contrast-enhanced CT to be an acceptable staging modality for pancreatic cancer [6]. It is possible that CT may have missed some small liver metastases that may have been detectable on MRI. We had only one CTTA reviewer in this

study. However, prior CTTA studies have shown good to excellent interobserver agreement [34, 35, 37–39].

In conclusion, metastatic disease at presentation has the most significant effect on overall survival in unresectable pancreas cancer. However, texture features are important in predicting outcomes in unresectable pancreas cancer. In particular, high mean positive pixel value and kurtosis at medium spatial filter are associated with poor prognosis. CT texture analysis may be a useful adjunct to contrast-enhanced CT in stratifying prognosis in patients with pancreas cancer, especially in those without metastatic disease at presentation.

Funding The authors state that this work has not received any funding.

Compliance with ethical standards

Guarantor The scientific guarantor of this publication is Kumaresan Sandrasegaran, M.D.

Conflict of interest The authors of this manuscript declare no relationships with any companies whose products or services may be related to the subject matter of the article.

Statistics and biometry A professor of Biostatistics (Dr Yan Tong, PhD) was consulted for specialist advice.

Informed consent Written informed consent was waived by the institutional review board.

Ethical approval Institutional review board approval was obtained.

Methodology

- Retrospective
- Case-control study
- Performed at one institution

References

1. Brosens LA, Hackeng WM, Offerhaus GJ, Hruban RH, Wood LD (2015) Pancreatic adenocarcinoma pathology: changing "landscape". *J Gastrointest Oncol* 6:358–374
2. Ethun CG, Kooby DA (2016) The importance of surgical margins in pancreatic cancer. *J Surg Oncol* 113:283–288

3. Hidalgo M, Cascinu S, Kleeff J et al (2015) Addressing the challenges of pancreatic cancer: future directions for improving outcomes. *Pancreatol* 15:8–18
4. Gall TM, Tsakok M, Wasan H, Jiao LR (2015) Pancreatic cancer: current management and treatment strategies. *Postgrad Med J* 91:601–607
5. Vincent A, Herman J, Schulick R, Hruban RH, Goggins M (2011) Pancreatic cancer. *Lancet* 378:607–620
6. Tempero MA, Malafa MP, Al-Hawary M et al (2017) Pancreatic adenocarcinoma, version 2.2017, NCCN clinical practice guidelines in oncology. *J Natl Compr Canc Netw* 15:1028–1061
7. Nelson DA, Tan TT, Rabson AB, Anderson D, Degenhardt K, White E (2004) Hypoxia and defective apoptosis drive genomic instability and tumorigenesis. *Genes Dev* 18:2095–2107
8. Marusyk A, Polyak K (2010) Tumor heterogeneity: causes and consequences. *Biochim Biophys Acta* 1805:105–117
9. Easwaran H, Tsai HC, Baylin SB (2014) Cancer epigenetics: tumor heterogeneity, plasticity of stem-like states, and drug resistance. *Mol Cell* 54:716–727
10. An FQ, Matsuda M, Fujii H et al (2001) Tumor heterogeneity in small hepatocellular carcinoma: analysis of tumor cell proliferation, expression and mutation of p53 AND beta-catenin. *Int J Cancer* 93:468–474
11. Yip C, Davnall F, Kozarski R et al (2015) Assessment of changes in tumor heterogeneity following neoadjuvant chemotherapy in primary esophageal cancer. *Dis Esophagus* 28:172–179
12. Yip C, Landau D, Kozarski R et al (2014) Primary esophageal cancer: heterogeneity as potential prognostic biomarker in patients treated with definitive chemotherapy and radiation therapy. *Radiology* 270:141–148
13. Gerlinger M, Rowan AJ, Horswell S et al (2012) Intratumor heterogeneity and branched evolution revealed by multiregion sequencing. *N Engl J Med* 366:883–892
14. Ng F, Kozarski R, Ganeshan B, Goh V (2013) Assessment of tumor heterogeneity by CT texture analysis: can the largest cross-sectional area be used as an alternative to whole tumor analysis? *Eur J Radiol* 82:342–348
15. Yip C, Tacelli N, Remy-Jardin M et al (2015) Imaging tumor response and tumoral heterogeneity in non-small cell lung cancer treated with antiangiogenic therapy: comparison of the prognostic ability of RECIST 1.1, an alternate method (Crabb), and image heterogeneity analysis. *J Thorac Imaging* 30:300–307
16. Ganeshan B, Burnand K, Young R, Chatwin C, Miles K (2011) Dynamic contrast-enhanced texture analysis of the liver: initial assessment in colorectal cancer. *Invest Radiol* 46:160–168
17. Davnall F, Yip CS, Ljungqvist G et al (2012) Assessment of tumor heterogeneity: an emerging imaging tool for clinical practice? *Insights Imaging* 3:573–589
18. Ng F, Ganeshan B, Kozarski R, Miles KA, Goh V (2013) Assessment of primary colorectal cancer heterogeneity by using whole-tumor texture analysis: contrast-enhanced CT texture as a biomarker of 5-year survival. *Radiology* 266:177–184
19. Bayanati H, E Thornhill R, Souza CA et al (2015) Quantitative CT texture and shape analysis: can it differentiate benign and malignant mediastinal lymph nodes in patients with primary lung cancer? *Eur Radiol* 25:480–487
20. Ganeshan B, Panayiotou E, Burnand K, Dizdarevic S, Miles K (2012) Tumour heterogeneity in non-small cell lung carcinoma assessed by CT texture analysis: a potential marker of survival. *Eur Radiol* 22:796–802
21. Ganeshan B, Skogen K, Pressney I, Coutroubis D, Miles K (2012) Tumour heterogeneity in oesophageal cancer assessed by CT texture analysis: preliminary evidence of an association with tumour metabolism, stage, and survival. *Clin Radiol* 67:157–164
22. Zhang H, Graham CM, Elci O et al (2013) Locally advanced squamous cell carcinoma of the head and neck: CT texture and histogram analysis allow independent prediction of overall survival in patients treated with induction chemotherapy. *Radiology* 269:801–809
23. Ahn SY, Park CM, Park SJ et al (2015) Prognostic value of computed tomography texture features in non-small cell lung cancers treated with definitive concomitant chemoradiotherapy. *Invest Radiol* 50:719–725
24. Goh V, Ganeshan B, Nathan P, Juttla JK, Vinayan A, Miles KA (2011) Assessment of response to tyrosine kinase inhibitors in metastatic renal cell cancer: CT texture as a predictive biomarker. *Radiology* 261:165–171
25. Tian F, Hayano K, Kambadakone AR, Sahani DV (2015) Response assessment to neoadjuvant therapy in soft tissue sarcomas: using CT texture analysis in comparison to tumor size, density, and perfusion. *Abdom Imaging* 40:1705–1712
26. Sandrasegaran KSA, Deng Y, Samuel A et al (2017) Usefulness of CT texture analysis in characterizing renal cancers. *Radiological Society of North America RSNA, Chicago, Ill*
27. Ganeshan B, Miles KA (2013) Quantifying tumour heterogeneity with CT. *Cancer Imaging* 13:140–149
28. Miles KA, Ganeshan B, Hayball MP (2013) CT texture analysis using the filtration-histogram method: what do the measurements mean? *Cancer Imaging* 13:400–406
29. Ganeshan B, Abaleke S, Young RC, Chatwin CR, Miles KA (2010) Texture analysis of non-small cell lung cancer on unenhanced computed tomography: initial evidence for a relationship with tumour glucose metabolism and stage. *Cancer Imaging* 10:137–143
30. Sasaguri K, Takahashi N, Gomez-Cardona D et al (2015) Small (<4 cm) renal mass: differentiation of oncocytoma from renal cell carcinoma on biphasic contrast-enhanced CT. *AJR Am J Roentgenol* 205:999–1007
31. Aickin M, Gensler H (1996) Adjusting for multiple testing when reporting research results: the Bonferroni vs Holm methods. *Am J Public Health* 86:726–728
32. Ganeshan B, Miles KA, Young RC, Chatwin CR (2007) Hepatic entropy and uniformity: additional parameters that can potentially increase the effectiveness of contrast enhancement during abdominal CT. *Clin Radiol* 62:761–768
33. Lubner MG, Stabo N, Lubner SJ et al (2015) CT textural analysis of hepatic metastatic colorectal cancer: pre-treatment tumor heterogeneity correlates with pathology and clinical outcomes. *Abdom Imaging* 40:2331–2337
34. Hayano K, Tian F, Kambadakone AR et al (2015) Texture analysis of non-contrast-enhanced computed tomography for assessing angiogenesis and survival of soft tissue sarcoma. *J Comput Assist Tomogr* 39:607–612
35. Smith AD, Gray MR, del Campo SM et al (2015) Predicting overall survival in patients with metastatic melanoma on antiangiogenic therapy and RECIST stable disease on initial posttherapy images using CT texture analysis. *AJR Am J Roentgenol* 205:W283–W293
36. Eilaghi A, Baig S, Zhang Y et al (2017) CT texture features are associated with overall survival in pancreatic ductal adenocarcinoma - a quantitative analysis. *BMC Med Imaging* 17:38
37. Hodgdon T, McInnes MD, Schieda N, Flood TA, Lamb L, Thornhill RE (2015) Can quantitative CT texture analysis be used to differentiate fat-poor renal angiomyolipoma from renal cell carcinoma on unenhanced CT images? *Radiology* 276:787–796
38. Schieda N, Thornhill RE, Al-Subhi M et al (2015) Diagnosis of sarcomatoid renal cell carcinoma with CT: evaluation by qualitative imaging features and texture analysis. *AJR Am J Roentgenol* 204:1013–1023
39. Takahashi N, Leng S, Kitajima K et al (2015) Small (< 4 cm) renal masses: differentiation of angiomyolipoma without visible fat from renal cell carcinoma using unenhanced and contrast-enhanced CT. *AJR Am J Roentgenol* 205:1194–1202